Chemical Engineering Journal 455 (2023) 140890

Contents lists available at ScienceDirect

Chemical Engineering Journal

journal homepage: www.elsevier.com/locate/cej

A multisensory-feedback tactile glove with dense coverage of sensing arrays for object recognition

Ye Qiu [a,b,c], Zhiqiang Wang [a,b,c], Pengcheng Zhu [a,d], Binbin Su [d], Chang Wei [a,d], Ye Tian [a,b,c], Zheng Zhang [a,b,c], Hao Chai [e], Aiping Liu [f], Lihua Liang [a,d,*], Huaping Wu [a,b,c,d,*]

[a] College of Mechanical Engineering, Zhejiang University of Technology, Hangzhou 310023, China
[b] Key Laboratory of Special Purpose Equipment and Advanced Processing Technology, Ministry of Education and Zhejiang Province, Zhejiang University of Technology, Hangzhou 310023, China
[c] Collaborative Innovation Center of High-end Laser Manufacturing Equipment (National "2011 Plan"), Zhejiang University of Technology, China
[d] Institute of Intelligent Manufacturing Technology and Equipment, Zhejiang University of Technology, Hangzhou 310018, China
[e] Zhijiang College of Zhejiang University of Technology, Shaoxing 312030, China
[f] Center for Optoelectronics Materials and Devices, Zhejiang Sci-Tech University, Hangzhou 310018, China

ARTICLE INFO

Keywords:
Tactile glove
Object recognition
Contact pressure
Thermal conductivity

ABSTRACT

Somatosensory networks that provide sophisticated sensory feedback and enable the dexterous manipulation of the human grasp remain difficult to replicate in robots, which is attributed to the grand challenge of densely covering the hand with tactile arrays. Here, a multisensory tactile glove is reported that is capable of object recognition with dense coverage of pressure and temperature sensing arrays. The synergistic effect of the multimodal configuration allows the tactile arrays to perceive contact pressure and thermal conductivity of an object involved in grasping motion, thus enhancing the accuracy via the combination of the mechanical features with thermal properties. By leveraging the multiple scanning technology and wireless transmission system, the tactile glove achieves a recognition accuracy of 94.2% in differentiating 20 types of objects with a modified deep learning algorithm. The large-area sensing arrays with high spatiotemporal resolution and multimodal sensing capabilities, which paves the way for the development of robot grasping tools, human–machine interfacing, and advanced prosthetics.

1. Introduction

Skin-based mechanoreceptors and thermoreceptors provide delicate sensory feedback for achieving environment awareness, threats recognition, and dexterous tasks [1,2]. Replicating the multimodal tactile perception capability in artificial skin enables the delicate manipulation of robotics and prosthetics, thus holding giant promise in human–machine interaction interfaces [3–7]. Although there has been significant progress in accumulatively understanding the underlying sensory mechanism and manufacturing technology [8–14], simultaneous implementation of precise mechanical and thermal sensing remains a daunting challenge yet. To realize object recognition with high accuracy in artificial tactile arrays, difficulties still exist in multifunctional integration, high spatiotemporal sensing resolution, and effective identifying methods.

Sophisticated tactile perception is important for achieving precise interaction with the environment, fine manipulation tasks, and artificial robot intelligent recognition [15–18]. The advancement of material modification and structure design in soft/flexible electronics has opened up new opportunities for the fabrication of devices that emulate tactile functions of the somatosensory system [19–28]. Tactile sensor arrays are constructed with diverse pressure sensing strategies (e.g., piezoresistive, piezoelectric, capacitive, and triboelectric) to extend into the desired pressure sensing matrix [29–38], thus holding the capability of tactile mapping in real-time. Moreover, efforts have been dedicated to extracting higher-level features from the sensing feedback signals, which further is utilized to realize the precise object identification with the assistance of algorithms [39–43]. However, pressure/force sensing is not sufficient to infer physical properties while substances with similar mechanical features, e.g., orange and tennis with similar softness, cannot be differentiated by only contact pressure. These tactile arrays with a single sensing mode impeded the fundamental grasping motion

* Corresponding authors at: College of Mechanical Engineering, Zhejiang University of Technology, Hangzhou 310018, China.
E-mail addresses: lianglihua@zjut.edu.cn (L. Liang), wuhuaping@gmaill.com (H. Wu).

https://doi.org/10.1016/j.cej.2022.140890
Received 11 July 2022; Received in revised form 14 September 2022; Accepted 7 December 2022
Available online 10 December 2022

based on complex object recognition, and therefore have exposed limitations in applications of minimally invasive surgery, industrial picking, and prosthetic rehabilitation.

To address these restrictions, additional efforts on combining the mechanical property with thermal features are explored to improve the recognition accuracy [44–50]. For instance, a tactile sensor with the integration of pressure and temperature sensing modules has been demonstrated to perceive contact pressure and thermal conductivity simultaneously, which can be applied to the robot hand for realizing garbage sorting [44]. Despite the notable progress has been achieved in the development of multifunctional tactile arrays, the sparse array distribution inevitably makes it a struggle to improve spatial resolution, thus rendering a great challenge to develop an artificial skin that is competent for the tactile distribution of complicated contact surfaces. The burdened elimination of mutual interference limits the simultaneous perception of multiple stimuli, resulting in poor sensing capability to decode complicated stimuli. Hence, it is highly desirable to develop and demonstrate a multimodal tactile array with high spatial resolution for future robots and human–machine interfaces.

Here, we report a multisensory array with dense coverage of pressure and temperature sensing modules that are further integrated by screen printing into a tactile glove covering the full hand, which is capable of simultaneously and independently perceiving contact pressure and thermal conductivity to realize precise object recognition. The synergistic effect of the multimodal configuration allows the arrayed tactile glove to distinguish the shape, pressure, temperature, and materials in a diverse set of objects. The tactile array assisted with the modified machine learning algorithm can effectively identify 20 kinds of objects with enhanced accuracy via the signal acquisition system. This smart glove reveals its potential as a promising solution for advanced human–machine interaction, which can benefit diversified areas, including artificial prosthetics, sorting industry, and microsurgery robots.

2. Experimental sections

2.1. Preparation of piezoresistive sensing material

In a preliminary synthesis procedure, the multi-wall carbon nanotubes (MWCNTs, Aladdin Tech. Inc), sodium dodecyl benzene sulfonate (SDBS) surfactant, SiO_2 nanoparticles, and silane coupling agent KH-560 are mixed with Cyclohexane at a 5:10:3:2:1000 wt ratio. Mechanical stirring at a temperature of 90 °C for 20 min to yield a uniform solution. Next, adding the silicone rubber GD401 (1 g) into the solution of Cyclohexane (25 mL) to acquire the hybrid under vigorous stirring for 30 min. The above two mixtures are poured into a beaker and sonicated for 30 min, followed by mechanical stirring for 1 h to get a uniform dispersion. After the mixed suspension turned viscous solution, the obtained solution was then put into the vacuum drying oven for 10 min to remove air bubbles.

2.2. Fabrication of multisensory tactile glove

The flexible printed circuit board (FPCB) with a 100 μm-thick polyimide was designed to the shape of a glove by Altium Designer according to the size of the human hand. Among them, the electrode size for the pressure sensing module is 4 mm × 4 mm, and the electrode for the temperature sensing module is evaporated with a size of 1 mm × 1 mm. Then, the pressure-sensing arrays are fabricated by screen printing using conductive piezoresistive sensing material on a FPCB and cured in the oven at 80 °C for 8 h (Fig. S1). The thickness of the printed piezoresistive material is 300 μm. After removing the screen-printing mask, the laser-cut adhesive layer with a thickness of 50 μm is attached to the top of the bottom electrode. The temperature sensing arrays (Negative Temperature Coefficient Thermistor, Fuwen sensing Co., ltd) were further integrated by spot welding. The dimension of the single temperature sensor used for the preparation of the tactile glove is 1 mm × 1 mm × 0.3 mm. In the end, the multisensory tactile glove was encapsulated with another FPCB to improve its robustness.

2.3. Measurements of the sensing performance of the sensors

To characterize the electrical response, the sensing signals from piezoresistive and temperature sensors were obtained using a semiconductor parameter analyzer (4200-SCS, Keithley). The pressure-loading tests were carried out using a mechanical testing system (INSTRON LEGEND2345).

2.4. Design of the data acquisition circuit

The designed circuit (Figs. S2 and S3) is comprised of a microcontroller Unit (MCU, nRF52832, Nordic), power supply (3.3 V and 2.048 V), channel selection (TMUX1108), analog switch (RS2105XN), and analog-to-digital converter (ADC, i.e., ADS1115). In brief, the PCB is designed to achieve the integrated function of data acquisition, signal processing, and signal transmission. The pressure and temperature sensing signals from the tactile glove are sampling in turn through the channel selection and analog switch module. Then the acquired sensing signals are processed by an ADC module and sent to the MCU, which are further transmitted to Bluetooth chip through serial communication with a baud rate 119200. The critical parameter of the hardware device in the tactile acquisition system is summarized in Table S1.

3. Results and discussion

3.1. Design of the multisensory tactile glove

Human skin is endowed with sensitivities to contact pressure and temperature to further infer the softness and material texture of the grasped object, which is attributed to the delicate and elaborate sensory receptors within dermal microstructures [51–54]. To mimic the physiological functions of mechanoreceptors and thermoreceptors of human skin, a multifunctional tactile array is demonstrated with flexible pressure and temperature sensing modules (Fig. 1a). The piezoresistive array is capable of decoding the softness and shape via the pressure mapping, whereas the thermo-sensitive array deposited on a polyimide substrate is utilized to differentiate the thermal conductivity. Combining mechanical features with the thermal property of an object and fusing the dual-mode sensing information, which enables enhanced recognition accuracy with the assistance of the machine learning models. The multisensory tactile array is integrated onto robotics to achieve precise object recognition (Fig. 1b), thus opening up new application opportunities for object recognition in interactive human–machine interfaces.

3.2. Property characterization of the pressure and temperature sensors

To evaluate the pressure-sensing performance of piezoresistive sensors, a quantitative analysis of piezoresistive output under pressure is carried out. The normalized relative resistance change ($\Delta R/R_0$, where R_0 refers to the initial resistance) of the piezoresistive layer as a function of the applied pressure, thereby showing its possibility to serve as a pressure sensor. More contacts among MWCNT are produced upon the compressive deformation, which increases the conduction paths and thus decreases the electrical resistance. The measuring results indicate that the demonstrated relative current change depends on the MWCNT concentration, which allows the sensing performance to be tuned by the content of MWCNT. In particular, the piezoresistive sensor with the 5 % MWCNT concentration exhibits an optimal sensitivity of 0.74 kPa^{-1} when the pressure is below 2 kPa and a sensitivity of 0.13 kPa^{-1} within the pressure range of 2–10 kPa (Fig. 2a). The excellent load-and-release performance has good reversibility and reliability repeated without a noticeable fluctuation in relative resistance change (Fig. 2b and S4a) after periodic cycles. The response and relaxation time of the

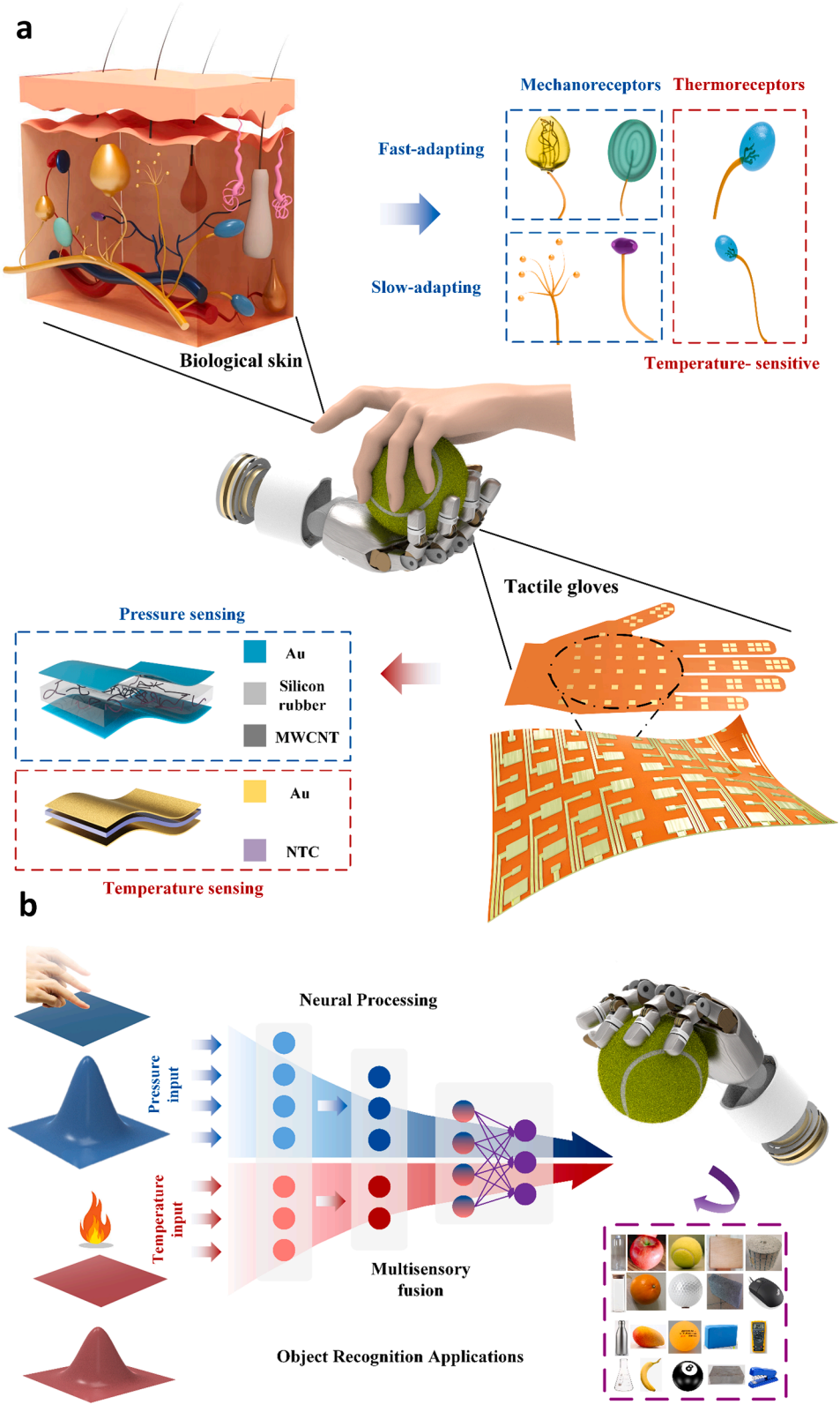

Fig. 1. Human skin-inspired tactile glove with object recognition capability. (a) Schematic illustrations of the structure of human skin and multisensory tactile glove. Human skin is composed of mechanoreceptors and thermoreceptors. The multisensory arrays consist of pressure and temperature sensing modules to perceive external stimuli. (b) The synergistic effect of multisensory feedback enables the manipulator to achieve the task of object recognition assisted with a deep convolutional neural network.

piezoresistive mode are determined to be 105 ms and 88 ms, respectively (Fig. 2c).

Besides the pressure-sensing performance, the capability of discriminating temperature is another important function for perceiving the external stimuli against the room temperature and improving environmental interaction. As expected, the relative resistance of the temperature sensor decreases with increasing environmental temperature range from 0 to 100 °C, showing a nearly linear temperature coefficient of resistance (TCR) of 0.17 $°C^{-1}$ within the temperature of 0–30 °C. In the high-temperature regime, the sensor exhibits a response with a sensitivity TCR of 0.95 $°C^{-1}$ (Fig. 2d). The response and relaxation time of the temperature mode are determined to be 194 ms and 928

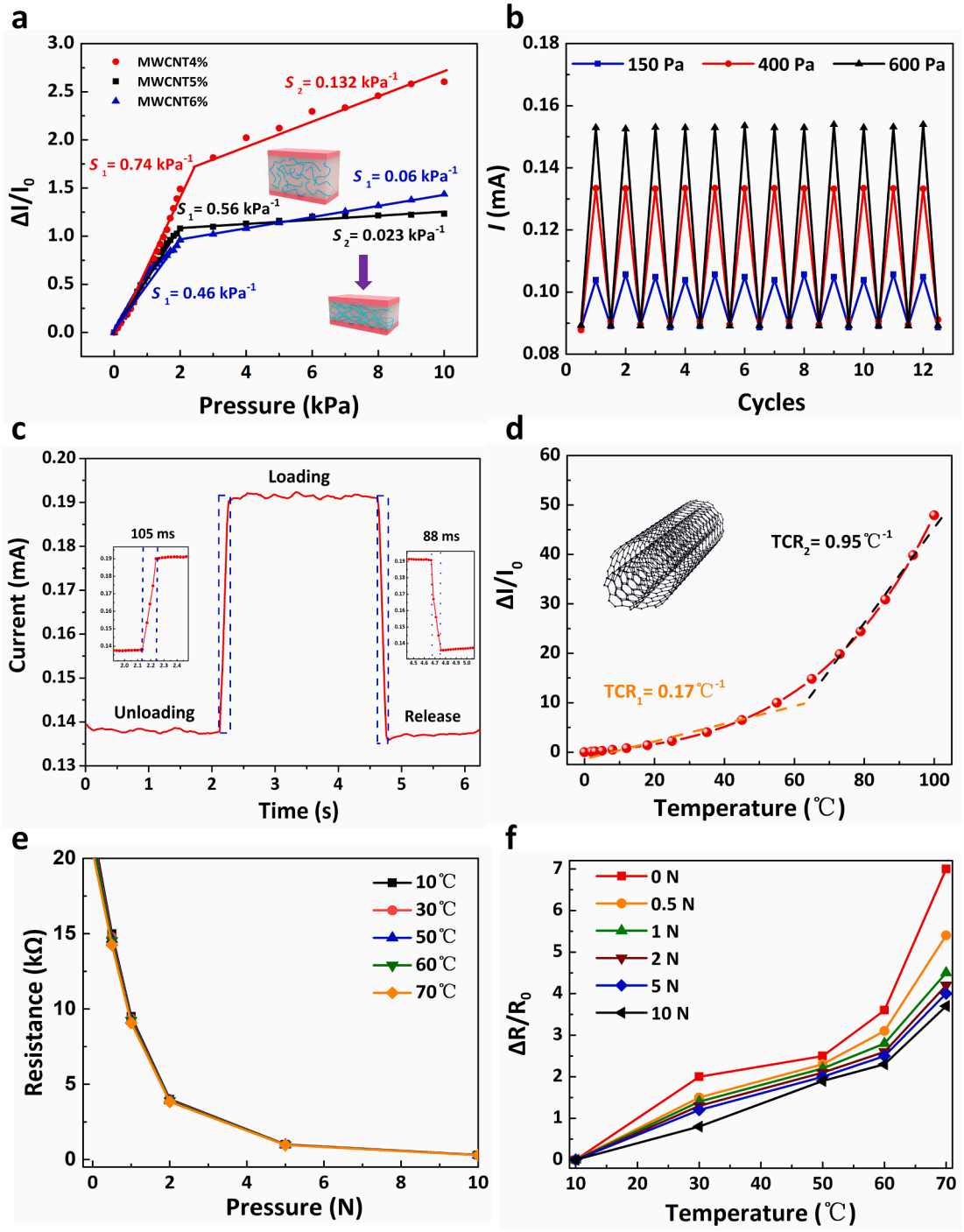

Fig. 2. The sensing performance of the multisensory tactile sensors. (a) The comparison of sensitivities of the piezoresistive layer with various MWCNT loading concentrations (4–6 %). (b) The real-time sensing response from the piezoresistive sensor for an applied pressure of 150 Pa, 400 Pa, and 600 Pa, respectively. (c) Determination of the response time for the piezoresistive sensor. (d) The resistance changes of the temperature sensor under various applied temperatures. (e) The resistance changes of the temperature sensor under various applied temperatures as a function of pressure. (f) The relative resistance changes of the temperature sensor under applied pressure range from 0 N to 10 N as a function of temperature.

ms, respectively (Fig. S5). The durability of the temperature sensor was tested by loading–unloading heat of 50 °C for over 1000 cycles, thereby demonstrating the reproducible and stable sensing performance (Fig. S4b). Moreover, stability under various levels of temperatures is also critical to practical applications since temperature inevitably affects the response of piezoresistive devices. The pressure-sensing capability over the temperature range of 10–70 °C reveals that the increasing temperature leads to a relative resistance change (Fig. 2e), which is attributed to the improved mobility of ions. The relative resistance change of pressure sensors affected by temperature is less than 7 % (Fig. 2f), making it a promising candidate for perception in complicated environments.

3.3. *Structural and acquiring method of the tactile glove*

As a primary verification of the multipixel-sensing function, a multifunctional tactile glove is designed based on the pressure and temperature arrays to explore the perceptual capability. To demonstrate

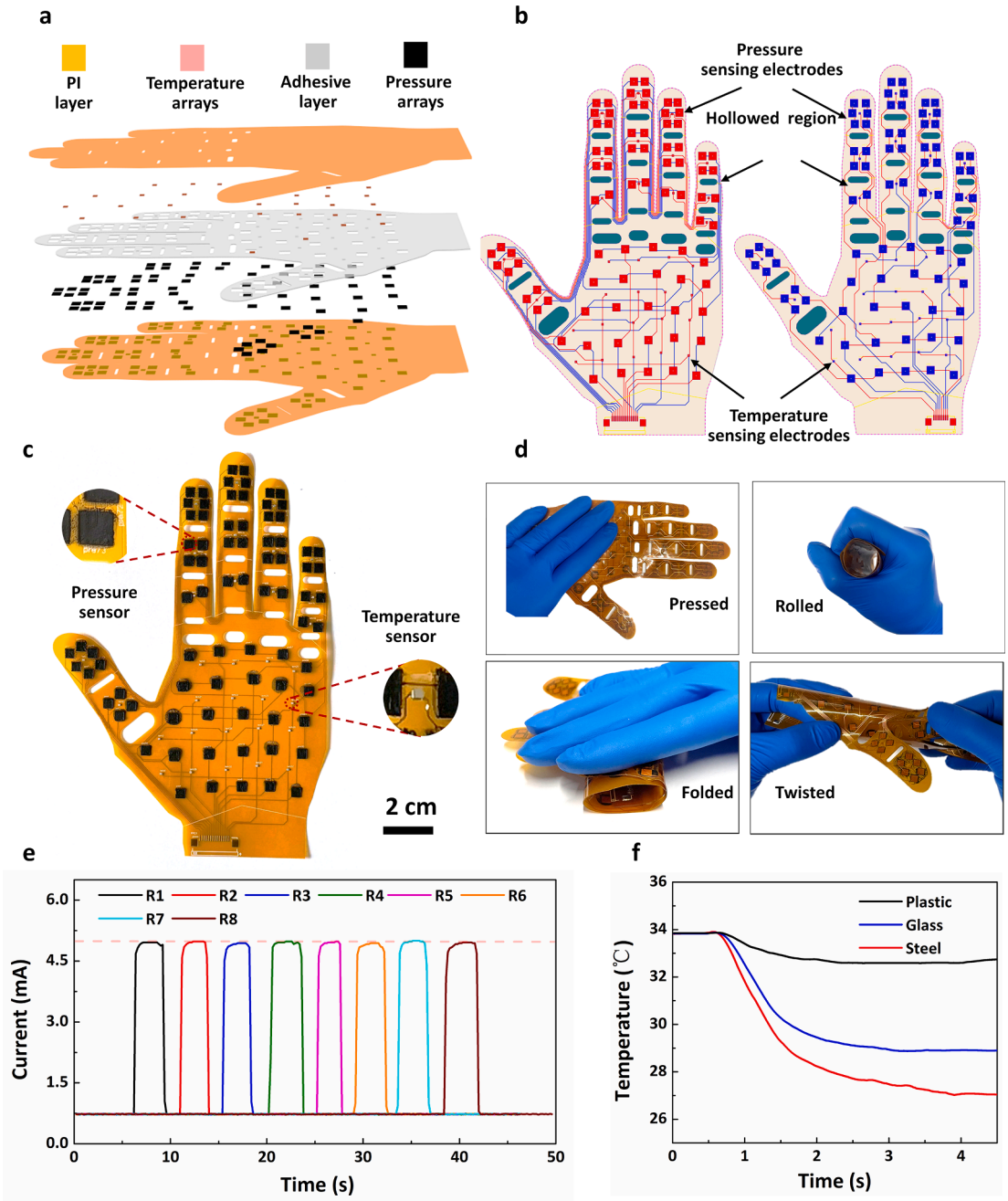

Fig. 3. The structural and acquiring method of the tactile glove. (a) Exploded overall structure of tactile glove comprising of FPCB, pressure arrays, adhesive layer, and temperature arrays. (b) The design of electrode arrays by using Altium Designer. (c) Photograph of a tactile glove with dense coverage of multisensory sensing arrays. (d) Photograph illustrates the flexibility of the tactile glove that can be pressed, rolled, folded, and twisted. (e) The current change of eight pressure sensing channels under pressure. (f) The real-time sensing response from the temperature sensor for touching objects of different materials.

the effect of the number of sensing points on the recognition accuracy, we have prepared three sensing arrays with various pressure elements (i.e., 2×2, 3×3, 4×4). The pressure distribution and recognition results (Fig. S6) indicate that sparser sensing arrays result in missing pressure mapping information of the object, thus reducing the recognition accuracy. Therefore, the designed tactile glove consists of 112 sensing elements to improve the identification accuracy (Fig. 3a). The pressure-sensing module (i.e., black) consists of 80 sensing elements and is capable of measuring the mechanical stimuli, whereas the temperature-sensing module (i.e., red) with 32 sensors to decode the thermal response. In virtue of the above structural design, distributed electrodes (Fig. 3b) are attached to the flat polyimide substrate through thermal evaporation, thus forming the FPCB layer. The screen-printed technology is then adopted to fabricate the pressure arrays made of MWCNT and silicone rubber possessing the piezoresistive characteristic, with a layer of silicone rubber covered on the top. Meanwhile, the temperature arrays composed of thermistors are further integrated via the method of spot welding. The as-fabricated sensing matrix (Fig. 3c) is encapsulated with a polyimide layer. In particular, the knuckle region of the tactile glove is hollowed out, so that there will be no restriction on bending deformation. Due to the flexibility of the above materials, the whole tactile array can be pressed, rolled, folded, and twisted with high adaptivity (Fig. 3d), thus facilitating a conformal and scalable tactile glove covering the full hand.

In addition to the significant role performed by the design of the array structure, an efficient and precise acquisition method of tactile

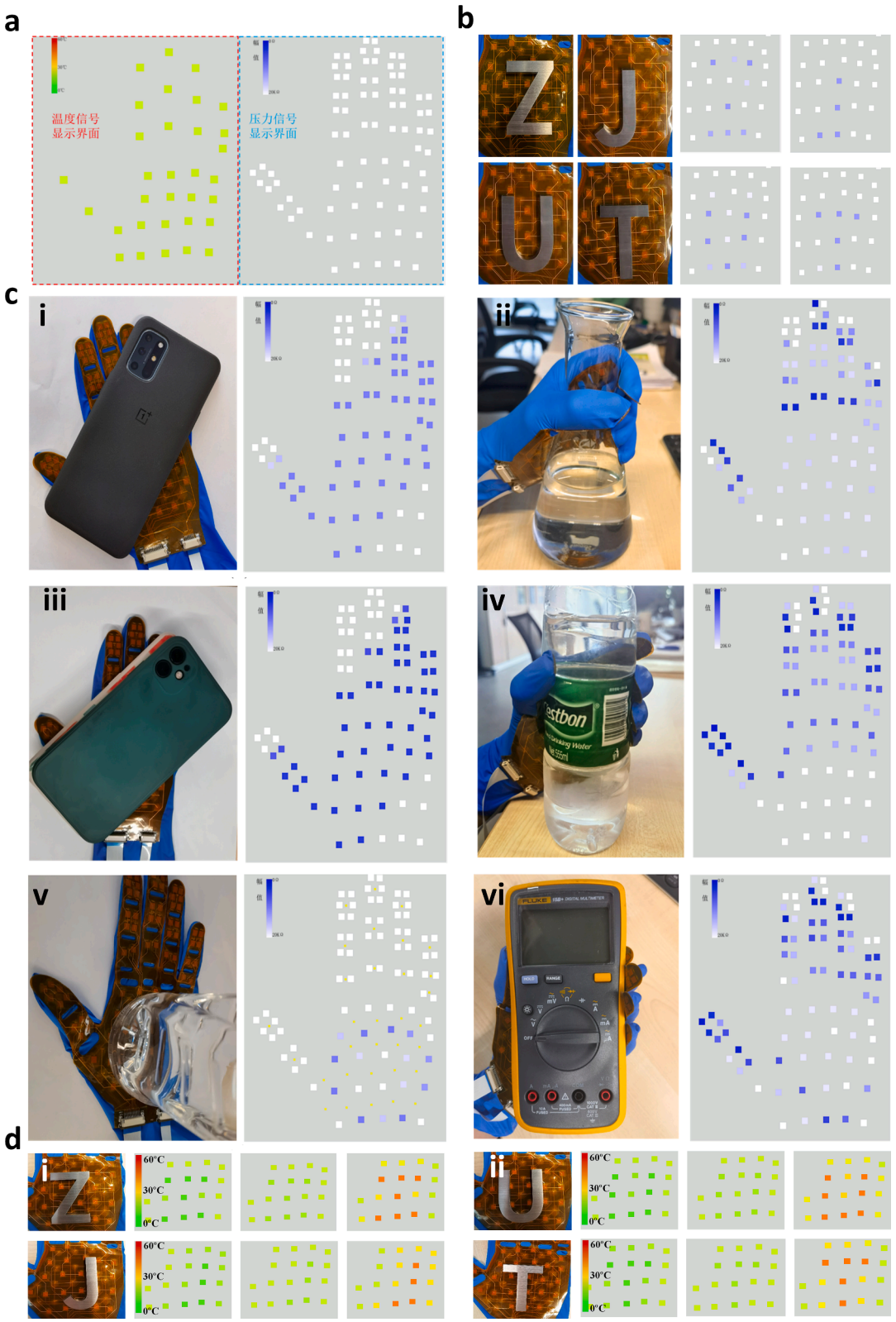

Fig. 4. Demonstration of pressure and temperature sensing functions of the tactile glove. (a) Photograph of the pressure and temperature distribution display. (b) The pressure distribution of four metal blocks. (c) The response of the tactile glove pressed and touched under various objects in daily life. (d) The temperature distribution of four metal blocks heated the temperature range from 10 °C to 45 °C.

arrays is particularly essential for avoiding crosstalk interferences in sensing signals. A multiple measuring resolution technology (Fig. S7) is demonstrated to achieve high-efficiency scanning, which eliminates crosstalk and reduces the power consumption through a few analog switches. For instance, crosstalk testing of the temperature array resistance network is performed using the multiple measuring resolution and the direct measuring method (Fig. S8), the comparative result reveals that eight sensing signals tested by the multiple measuring technology provide accurate feedback of temperature changes without interference between them. Compared to the conventional secondary measuring method that requires $2 \times n \times m$ scanning for $n \times m$ sensing units (n is the row and m is the column), numbers of scans for only $n \times m$ are needed in the proposed multiple testing strategy, thus simplifying the circuit design and removing the necessity of negative power supply, operational amplifier, and other electronic devices. Therefore, this developed scanning technology allows for large area integrated sensing arrays with high resolution.

To further validate the reliability of the signal acquiring technology, the pressure sensing test of the single-pixel sensor is firstly performed under press cycles ranging from 20 g to 100 g, indicating a stable sensing performance collected via the multiple scanning (Fig. S9). Based on the excellent capabilities of a single sensing unit, the homogeneity test of multipixel tactile arrays is subsequently carried out on eight sensing modules, from which we can see the consistency of current response of the tactile sensor array under the same stimulus (Fig. 3e). The evaluation of the temperature sensing performance through the proposed acquisition system is equally important, so objects of three different materials (i.e., stainless steel, plastic, and wood) are sequentially touched to the tactile glove to obtain the temperature profile over time (Fig. 3f). The temperature of the object made of stainless steel varies from 34 °C to 27 °C within 4 s, and the rate of temperature change is significantly faster than the other two material objects. The mechanism of using temperature sensors for object recognition lies in the detected the speed of temperature change of the contact object with various thermal conductivities to distinguish the material of the object. When the above three materials contact the temperature sensor, the conductive heat transfer from the sensor to its surroundings changes with the thermal conductivity of the objects. Hence, the thermal conductivity of different materials can be evaluated by identifying the temperature variation of the sensing unit, thus making it possible to differentiate between different materials.

3.4. Object recognition assisted by the deep learning algorithm

Upon the excellent sensing performance and efficient signal acquiring method, the tactile glove with integrated pressure and temperature sensing arrays can be employed to explore the high-density mapping capabilities. The corresponding tactile signal display interface is further designed and developed to intuitively reveal the spatial resolution of tactile glove (Fig. 4a). As the four metal alphabet blocks (i.e., ZJUT) are placed sequentially in the palm area of the tactile glove, apparent resistance changes from the corresponding pixels were collected and reproduced in pressure distribution images to determine the position and pressure magnitude (Fig. 4b). To further investigate the multipixel sensing capability of the tactile system when grasping an object in daily routine, various types of objects (e.g., smartphone, water bottle) are placed on top of the sensing array to demonstrate the pressure distribution generated by the loading (Fig. 4c), which is consistent with the shape of the displaced objects. Besides, the position where the objects with different curved surfaces is put has a significant change in resistance, and the magnitude and location of the pressure could also be recognized from the sensing mapping. Simultaneous multipixel pressure and temperature sensing are of great importance to giving effective feedback and achieving precise recognition. The measured temperature distribution agrees with the profile of the object shape, and the displayed temperature also matches the actual applied temperature to the metal alphabet blocks (Fig. 4d). These measuring results indicate the tactile arrays with high spatiotemporal resolution and multimodal sensing abilities, which facilitates the promising object-identifying application of the wearable tactile devices.

Incorporating neural networks and deep learning with tactile sensors to extend the capability of accurate real-time object recognition. A tactile dataset is constructed from the 20 objects containing five categories (i.e., containers, fruits, balls, blocks, and daily necessities) with diverse sizes, shapes, and materials (Fig. 5a). Testing signals are acquired by collecting circuits and then converted into pixels by normalizing to the range of 0 to 255 and transformed as a $25 \times 32 \times 32$ image corresponding to their locations (Fig. 5b). The whole data (containing 30 sets, 112 sets for each object) is divided into a training set (70 %) and a testing set (30 %) to train a convolutional neural network (CNN) model. Considering the multidimensional and enormous data acquired from the dual-mode sensing arrays, the CNN deep-learning algorithm is designed to conduct classification in the PyTorch framework (Fig. 5c). In particular, the reason for utilizing LeNet model as a foundational framework is because of its simplicity and reliability for automatically extracting features, as well as it is known for high performance in image classification. Representative strategies to modify this conventional LeNet architecture include 1) employing the residual learning connection; 2) increasing the Batch Normalization layer and using LeakyReLU as the activation function to accelerate the convergence speed of the model; 3) exploiting 1×1 convolutional layers instead of fully connected layers to improve algorithm efficiency.

The modified LeNet model shows a faster error reduction compared to that of LeNet network with traditional architecture (Fig. S10), where the error magnitude is reduced to 0.02315 after 200 training steps. The confusion map utilizing only pressure sensing feedback shows that the total classification accuracy reaches about 85.65 % (Fig. 5d-I). However, the pressure sensing module cannot accurately discriminate objects with similar sizes, shapes, and softness but with different materials. The incorporation of pressure sensing with temperature sensing can improve the object recognition accuracy to about 94.9 % (Fig. 5d-II), which combines mechanical features with thermal properties. The classification results of various objects further confirm that exploring the relationship between temperature change and object material can effectively make up for the incompleteness of single pressure-sensing feedback, indicating it is feasible to utilize the multisensory tactile glove to recognize objects.

3.5. Applications of multisensory tactile gloves on the object recognition

The rapid development of multisensory electronic skins paves a way for the diversified application in object recognition, robot grasping tools, and human-robot interactions. Precisely capturing the real-time multidimensional stimuli creates application opportunities for identification scenarios, and here we demonstrate a tactile glove with dense coverage of pressure/temperature sensing arrays. The complete real-time recognition system includes the tactile glove, signal preprocessing circuit, MCU with wireless transmitter module, PC, and the display interface (Fig. 6a). In brief, the acquired sensing signals from the tactile arrays are processed by an analog-to-digital converter (ADC) after amplification and filtering out the ambient noise. Next, the MCU further receives digital signals from the ADC module, which are then sent to a workstation PC via a wireless transmission. Based on the received spectrum of signals, the PC will output the final recognition results through the assistance of a trained machine learning model. The time taken to transfer the data to the convolutional neural network model on PC to calculate the result is about 21 ms. The corresponding interface design of the object recognition consists of tactile signal display, serial communication, data acquisition, and object recognition results (Fig. 6b), which is developed to enable the visualization of object recognition results. Simultaneously, the integrated broadcast module will announce the corresponding prediction result after the tactile signal

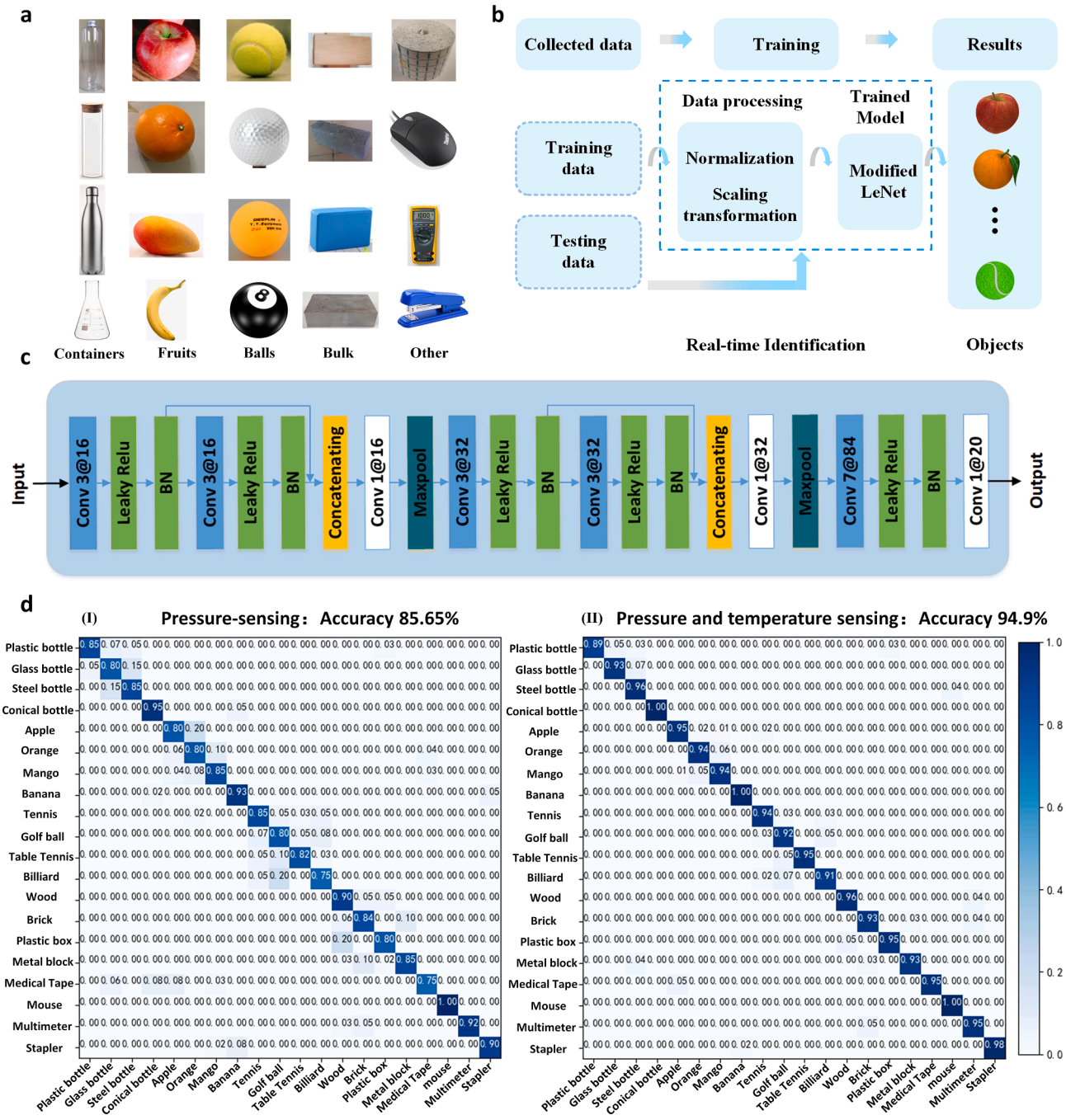

Fig. 5. Object identification of deep learning-enabled tactile glove. (a) Photograph of 20 objects used in the dataset. (b) Schematics of the process for training and real-time identification. (c) The CNN architecture constructed for identifying objects from tactile information input. (d) Classification test confusion matrix of object recognition derived from the (I) pressuring-sensing arrays and (II) pressure–temperature multisensory signals.

is analyzed via the training model.

For a practical demonstration toward the future application of object recognition, a multimodal tactile array composed of pressure and temperature sensing modules is equipped with rubber gloves, and further is integrated into the human hand to mimic the grasping motion of the prosthetic. The participant initially touches the object for the temperature sensing module on the tactile glove to reach thermal equilibrium with the human hand before carrying out the grasping action. Afterwards, the participant executes a stable grasping task of the measured object to obtain multisensory feedback information, which is further utilized to gain recognition results from the acquisition system. The corresponding spatial mapping of temperature and pressure are synchronously displayed on the screen of the PC, analyzing the softness and material of various objects through the real-time distribution to imply the tennis grasped in this motion (Fig. 6c). The identification result is announced by voice module within the recognition system, leading to a gentle release of the object for the next round of operation. Besides, the duration of the whole process of the haptic glove from grasping the object to the voice broadcast of the recognition result is 5 s (Video S1), demonstrating an efficient capability to recognize objects.

To further verify the functionality of the tactile glove, altogether 10 voluntary participants conduct object recognition tests with the overall accuracy in differentiating 20 types of objects up to 94.2 % (Table S2), which is close to the classification accuracy of the test set (94.9 %). Compared to object identification in literatures [55–58,39,44,46] (Table. S3), the presented tactile glove shows a remarkable capability of

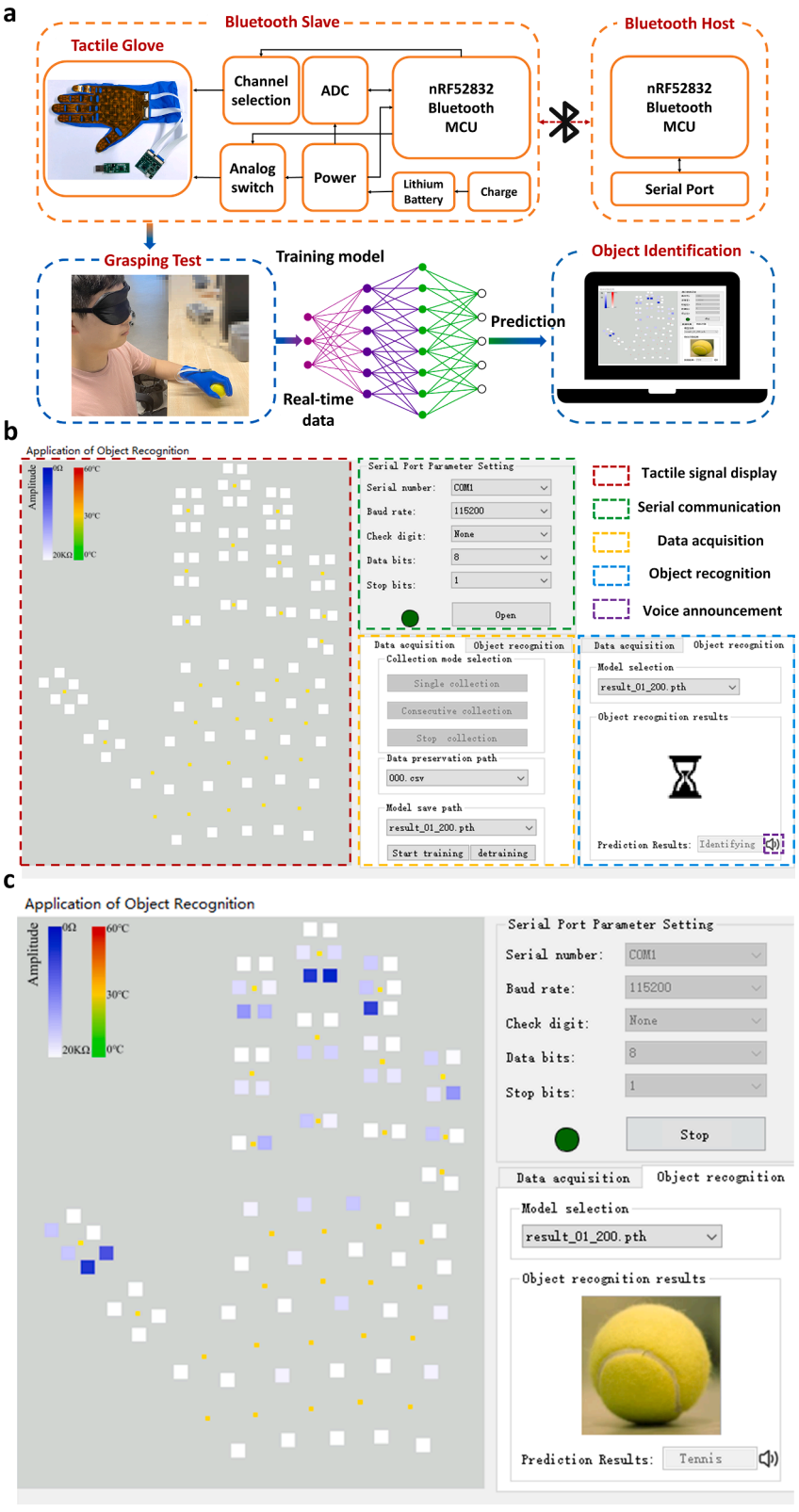

Fig. 6. Integrated demonstration of object recognition application. (a) Schematic diagram of the recognition system and process for classification with feature visualization. (b) The interface design of object recognition system is based on the multisensory arrays. (c) Real-time presentation of object recognition results.

possessing excellent recognition accuracy. This breakthrough behavior benefits from the combination of pressure and temperature arrays with high spatiotemporal sensing resolution, which is utilized to decode the softness and material of measured objects. We will further explore the integration of sensing arrays on robotic gripper to eliminate the multiple interferences during grasping motion and thus achieve accurate object recognition. On the basis of this proof of concept, the integration of tactile glove onto a robot hand will extend the utility of multisensory tactile arrays in dexterous tasks that require multi-information feedback. This work demonstrates the tactile glove covering the full hand

with high-density multisensory sensing arrays, providing crucial strategies for the tremendous potentials of intelligent sorting, prosthetics, and humanoid robotics.

4. Conclusions

In summary, we demonstrated a high-density tactile glove that is based on a screen-printed, multisensory array and has precise object recognition capabilities. The integrated pressure-sensing module works as mechanoreceptor with the ability to perceive contact pressure of grasped object, whereas the thermal conductivity of a material is recognized through the temperature-sensitive module to mimic the functional characteristics of the thermoreceptor. Simultaneous perception of the mechanical feature with thermal property, which facilitates the tactile glove with enhanced identification accuracy. By utilizing the multiple scanning technology, the signal acquiring method is capable of effectively eliminating crosstalk and reducing the power consumption assisted by the wireless transmission system. Through the integrated demonstration of object recognition application, 94.2 % accuracy of differentiating 20 kinds of grasped objects among ten participants has been achieved with deep learning analytics. The developed tactile glove reveals its potential as a promising solution for facilitating the dense coverage of sensing arrays with high spatiotemporal resolution and multimodal sensing abilities, which can benefit diversified areas, including microsurgery robots, human–machine interfacing, and advanced prosthetics.

Declaration of Competing Interest

The authors declare that they have no known competing financial interests or personal relationships that could have appeared to influence the work reported in this paper.

Data availability

Data will be made available on request.

Acknowledgments

This work was supported by the National Natural Science Foundation of China (Grant no. 11672269, 11972323, and 12002308); China Postdoctoral Science Foundation (Grant no. 2022M710129); Zhejiang Provincial Natural Science Foundation of China (Grant no. LQ22A020009, LR20A020002, LR19E020004, LR18E050002, LZY21E030002, LD21F030002, and LD22A020001); and Fundamental Research Funds for the Provincial Universities of Zhejiang (RF-B2019004); 111 Project (No.: D16004).

Appendix A. Supplementary data

Supplementary data to this article can be found online at https://doi.org/10.1016/j.cej.2022.140890.

References

[1] C.M. Boutry, M. Negre, M. Jorda, O. Vardoulis, A. Chortos, O. Khatib, Z. Bao, A hierarchically patterned, bioinspired e-skin able to detect the direction of applied pressure for robotics, Sci. Robot. 3 (24) (2018) eaau6914.
[2] J. Kim, M. Lee, H.J. Shim, R. Ghaffari, H.R. Cho, D. Son, Y.H. Jung, M. Soh, C. Choi, S. Jung, K. Chu, D. Jeon, S.T. Lee, J.H. Kim, S.H. Choi, T. Hyeon, D.H. Kim, Stretchable silicon nanoribbon electronics for skin prosthesis, Nat. Commun. 5 (2014) 5747.
[3] X. Chen, T. Wang, J. Shi, W. Lv, Y. Han, M. Zeng, J. Yang, N. Hu, Y. Su, H. Wei, Z. Zhou, Z. Yang, Y. Zhang, A Novel Artificial neuron-like gas sensor constructed from CuS quantum dots/Bi2S3 nanosheets, Nano-micro Lett. 14 (1) (2021) 8.
[4] Z.R. Zhai, Y. Wang, K. Lin, L.L. Wu, H.Q. Jiang, In situ stiffness manipulation using elegant curved origami, Sci. Adv. 6 (47) (2020) eabe2000.
[5] C.Q. Shi, Z.N. Zou, Z.P. Lei, P.C. Zhu, W. Zhang, J.L. Xiao, Heterogeneous integration of rigid, soft, and liquid materials for self-healable, recyclable, and reconfigurable wearable electronics, Sci. Adv. 6 (45) (2020) eabd0202.
[6] J. Hu, Y. Qiu, X. Wang, L. Jiang, X. Lu, M. Li, Z. Wang, K. Pang, Y. Tian, W. Zhang, Z. Xu, H. Zhang, H. Qi, A. Liu, Z. Zhang, H. Wu, Flexible six-dimensional force sensor inspired by the tenon-and-mortise structure of ancient Chinese architecture for orthodontics, Nano Energy 96 (2022).
[7] S.M. Won, H. Wang, B.H. Kim, K. Lee, H. Jang, K. Kwon, M. Han, K.E. Crawford, H. Li, Y. Lee, X. Yuan, S.B. Kim, Y.S. Oh, W.J. Jang, J.Y. Lee, S. Han, J. Kim, X. Wang, Z. Xie, Y. Zhang, Y. Huang, J.A. Rogers, Multimodal sensing with a three-dimensional piezoresistive structure, ACS Nano 13 (10) (2019) 10972–10979.
[8] L. Tian, B. Zimmerman, A. Akhtar, K.J. Yu, M. Moore, J. Wu, R.J. Larsen, J.W. Lee, J. Li, Y. Liu, B. Metzger, S. Qu, X. Guo, K.E. Mathewson, J.A. Fan, J. Cornman, M. Fatina, Z. Xie, Y. Ma, J. Zhang, Y. Zhang, F. Dolcos, M. Fabiani, G. Gratton, T. Bretl, L.J. Hargrove, P.V. Braun, Y. Huang, J.A. Rogers, Large-area MRI-compatible epidermal electronic interfaces for prosthetic control and cognitive monitoring, Nat. Biomed. Eng. 3 (3) 3 (2019) 194-205.
[9] Y.C. Zhang, N. Zheng, Y. Cao, F.L. Wang, P. Wang, Y.J. Ma, B.W. Lu, G.H. Hou, Z. Z. Fang, Z.W. Liang, M.K. Yue, Y. Li, Y. Chen, J. Fu, J. Wu, T. Xie, X. Feng, Climbing-inspired twining electrodes using shape memory for peripheral nerve stimulation and recording, Sci. Adv. 5 (4) (2019) eaaw1066.
[10] Z. Cui, W. Wang, L. Guo, Z. Liu, P. Cai, Y. Cui, T. Wang, C. Wang, M. Zhu, Y. Zhou, W. Liu, Y. Zheng, G. Deng, C. Xu, X. Chen, Haptically quantifying young's modulus of soft materials using a self-locked stretchable strain sensor, Adv. Mater. (2021) e2104078.
[11] Y. Wang, T. Tang, Y. Xu, Y. Bai, L. Yin, G. Li, H. Zhang, H. Liu, Y. Huang, All-weather, natural silent speech recognition via machine-learning-assisted tattoo-like electronics, npj Flex, Electron. 5 (1) (2021) 20.
[12] S. Pyo, J. Lee, K. Bae, S. Sim, J. Kim, Recent progress in flexible tactile sensors for human-interactive systems: from sensors to advanced applications, Adv. Mater. 33 (47) (2021) e2005902.
[13] F. Zhang, P.C. Ma, J. Wang, Q. Zhang, W. Feng, Y. Zhu, Q. Zheng, Anisotropic conductive networks for multidimensional sensing, Mater. Horiz. 8 (10) (2021) 2615–2653.
[14] C.J. Wang, C.H. Linghu, S. Nie, C.L. Li, Q.J. Lei, X. Tao, Y.J. Zeng, Y.P. Du, S. Zhang, K.X. Yu, H. Jin, W.Q. Chen, J.Z. Song, Programmable and scalable transfer printing with high reliability and efficiency for flexible inorganic electronics, Sci. Adv. 6 (25) (2020) eabb2393.
[15] T.Y. Fan, Z.Y. Liu, Z.W. Luo, J.D. Li, X.Y. Tian, Y.S. Chen, Y. Feng, C.L. Wang, H. C. Bi, X.M. Li, F. Qiao, X. Wu, Analog sensing and computing systems with low power consumption for gesture recognition, Adv. Intell. Syst. 3 (1) (2021) 2000184.
[16] W.L. Li, N. Matsuhisa, Z.Y. Liu, M. Wang, Y.F. Luo, P.Q. Cai, G. Chen, F.L. Zhang, C. C. Li, Z.H. Liu, Z.S. Lv, W. Zhang, X.D. Chen, An on-demand plant-based actuator created using conformable electrodes, Nat. Electron. 4 (2) (2021) 134–142.
[17] X.Y. Tian, Z.Y. Liu, Z.W. Luo, X. Wu, F. Qiao, X.W. Wang, G.H. Li, J. Wu, J. Zhang, Z. Liu, J.H. Chu, Dual-mode sensor and actuator to learn human-hand tracking and grasping, IEEE Trans. Electron. Dev. 66 (12) (2019) 5407–5410.
[18] N. Li, Z.H. Yin, W.G. Zhang, C.Y. Xing, T.J. Peng, B. Meng, J. Yang, Z.C. Peng, A triboelectric-inductive hybrid tactile sensor for highly accurate object recognition, Nano Energy 96 (2022), 107063.
[19] C.H. Wang, X.S. Li, H.J. Hu, L. Zhang, Z.L. Huang, M.Y. Lin, Z.R. Zhang, Z.N. Yin, B. Huang, H. Gong, S. Bhaskaran, Y. Gu, M. Makihata, Y.X. Guo, Y.S. Lei, Y. M. Chen, C.F. Wang, Y. Li, T.J. Zhang, Z.Y. Chen, A.P. Pisano, L.F. Zhang, Q. F. Zhou, S. Xu, Monitoring of the central blood pressure waveform via a conformal ultrasonic device, Nat. Biomed. Eng. 2 (9) (2018) 687–695.
[20] Y.C. Lai, J. Deng, R. Liu, Y.C. Hsiao, S.L. Zhang, W. Peng, H.M. Wu, X. Wang, Z. L. Wang, Actively perceiving and responsive soft robots enabled by self-powered, highly extensible, and highly sensitive triboelectric proximity- and pressure-sensing skins, Adv. Mater. 30 (28) (2018) e1801114.
[21] C. Zhang, H. Zheng, J. Sun, Y. Zhou, W. Xu, Y. Dai, J. Mo, Z. Wang, 3D Printed, Solid-State Conductive Ionoelastomer as a Generic Building Block for Tactile Applications, Adv. Mater. 34 (2) (2021) e2105996.
[22] C. Wang, K. Sim, J. Chen, H. Kim, Z. Rao, Y. Li, W. Chen, J. Song, R. Verduzco, C. Yu, Soft ultrathin electronics innervated adaptive fully soft robots, Adv. Mater. 30 (13) (2018) 1706695.
[23] Y. Qiu, C. Wang, X. Lu, H. Wu, X. Ma, J. Hu, H. Qi, Y. Tian, Z. Zhang, G. Bao, H. Chai, J. Song, A. Liu, A Biomimetic drosera capensis with adaptive decision-predation behavior based on multifunctional sensing and fast actuating capability, Adv. Funct. Mater. 32 (13) (2021) 2110296.
[24] N.N. Bai, L. Wang, Q. Wang, J. Deng, Y. Wang, P. Lu, J. Huang, G. Li, Y. Zhang, J. L. Yang, K.W. Xie, X.H. Zhao, C.F. Guo, Graded intrafillable architecture-based iontronic pressure sensor with ultra-broad-range high sensitivity, Nat. Commun. 11 (1) (2020) 209.
[25] Z. Wang, L. Wang, Y. Wu, L. Bian, M. Nagai, R. Jv, L. Xie, H. Ling, Q. Li, H. Bian, M. Yi, N. Shi, X. Liu, W. Huang, Signal filtering enabled by spike voltage-dependent plasticity in metalloporphyrin-based memristors, Adv. Mater. 33 (43) (2021) 2104370.
[26] C. Qu, S. Wang, L. Liu, Y. Bai, L. Li, F. Sun, M. Hao, T. Li, Q. Lu, L. Li, S. Qin, T. Zhang, Bioinspired flexible volatile organic compounds sensor based on dynamic surface wrinkling with dual-signal response, Small 15 (17) (2019) 1900216.
[27] Y. Qiu, S. Sun, C. Xu, Y. Wang, Y. Tian, A. Liu, X. Hou, H. Chai, Z. Zhang, H. Wu, The frequency-response behaviour of flexible piezoelectric devices for detecting the magnitude and loading rate of stimuli, J. Mater. Chem. C 9 (2) (2021) 584–594.

[28] H. Zhou, Y. Zhang, Y. Qiu, H. Wu, W. Qin, Y. Liao, Q. Yu, H. Cheng, Stretchable piezoelectric energy harvesters and self-powered sensors for wearable and implantable devices, Biosens. Bioelectron. 168 (2020), 112569.
[29] C. Wang, M. Cai, Z. Hao, S. Nie, C. Liu, H. Du, J. Wang, W. Chen, J. Song, Stretchable, multifunctional epidermal sensor patch for surface electromyography and strain measurements, Adv. Intell. Syst. 3 (11) (2021) 2100031.
[30] D. Yan, J. Chang, H. Zhang, J. Liu, H. Song, Z. Xue, F. Zhang, Y. Zhang, Soft three-dimensional network materials with rational bio-mimetic designs, Nat. Commun. 11 (1) (2020) 1180.
[31] Y. Tian, J. Han, J. Yang, H. Wu, H. Bai, A Highly Sensitive Graphene Aerogel Pressure Sensor Inspired by Fluffy Spider Leg, Adv. Mater. Interfaces. 8 (15) (2021) 2100511.
[32] M. Zhu, M. Lou, I. Abdalla, J. Yu, Z. Li, B. Ding, Highly shape adaptive fiber based electronic skin for sensitive joint motion monitoring and tactile sensing, Nano Energy 69 (2020), 104429.
[33] C. Wan, P. Cai, X. Guo, M. Wang, N. Matsuhisa, L. Yang, Z. Lv, Y. Luo, X.J. Loh, X. Chen, An artificial sensory neuron with visual-haptic fusion, Nat. Commun. 11 (1) (2020) 4602.
[34] M.L. Zhu, Z.D. Sun, Z.X. Zhang, Q.F. Shi, T.Y.Y. He, H.C. Liu, T. Chen, C.K. Lee, Haptic-feedback smart glove as a creative human-machine interface (HMI) for virtual/augmented reality applications, Sci. Adv. 6 (19) (2020) eaaz8693.
[35] L. Li, J. Zheng, J. Chen, Z. Luo, Y. Su, W. Tang, X. Gao, Y. Li, C. Cao, Q. Liu, X. Kang, L. Wang, H. Li, Flexible Pressure Sensors for Biomedical Applications: From Ex Vivo to In Vivo, Adv. Mater. Interfaces. 7 (17) (2020) 2000743.
[36] H. Chen, Y. Jing, J.-H. Lee, D. Liu, J. Kim, S. Chen, K. Huang, X. Shen, Q. Zheng, J. Yang, S. Jeon, J.-K. Kim, Human skin-inspired integrated multidimensional sensors based on highly anisotropic structures, Mater. Horiz. 7 (9) (2020) 2378–2389.
[37] H. Wu, H. Qi, X. Wang, Y. Qiu, K. Shi, H. Zhang, Z. Zhang, W. Zhang, Y. Tian, Stretchable, sensitive, flexible strain sensor incorporated with patterned liquid metal on hydrogel for human motion monitoring and human–machine interaction, J. Mater. Chem. C 10 (21) (2022) 8206–8217.
[38] H. Tan, Q. Tao, I. Pande, S. Majumdar, F. Liu, Y. Zhou, P.O.A. Persson, J. Rosen, S. van Dijken, Tactile sensory coding and learning with bio-inspired optoelectronic spiking afferent nerves, Nat. Commun. 11 (1) (2020) 1369.
[39] S. Sundaram, P. Kellnhofer, Y. Li, J.Y. Zhu, A. Torralba, W. Matusik, Learning the signatures of the human grasp using a scalable tactile glove, Nature 569 (7758) (2019) 698–702.
[40] D. Liu, D. Zhang, Z. Sun, S. Zhou, W. Li, C. Li, W. Li, W. Tang, Z.L. Wang, Active-matrix sensing array assisted with machine-learning approach for lumbar degenerative disease diagnosis and postoperative assessment, Adv. Funct. Mater. 32 (21) (2022) 2113008.
[41] A. Moin, A. Zhou, A. Rahimi, A. Menon, S. Benatti, G. Alexandrov, S. Tamakloe, J. Ting, N. Yamamoto, Y. Khan, F. Burghardt, L. Benini, A.C. Arias, J.M. Rabaey, A wearable biosensing system with in-sensor adaptive machine learning for hand gesture recognition, Nature Electronics 4 (1) (2020) 54–63.
[42] K. Pang, X. Song, Z. Xu, X.T. Liu, Y.J. Liu, L. Zhong, Y.X. Peng, J.X. Wang, J. Z. Zhou, F.X. Meng, J. Wang, C. Gao, Hydroplastic foaming of graphene aerogels and artificially intelligent tactile sensors, Sci. Adv. 6 (46) (2020) eabd4045.
[43] Y. Luo, X. Xiao, J. Chen, Q. Li, H. Fu, Machine-learning-assisted recognition on bioinspired soft sensor arrays, ACS Nano (2022).
[44] G.Z. Li, S.Q. Liu, L.Q. Wang, R. Zhu, Skin-inspired quadruple tactile sensors integrated on a robot hand enable object recognition, Sci. Robot. 5 (49) (2020) eabc8134.
[45] H. Chen, J. Huang, J. Liu, J. Gu, J. Zhu, B. Huang, J. Bai, J. Guo, X. Yang, L. Guan, High toughness multifunctional organic hydrogels for flexible strain and temperature sensor, J. Mater. Chem. A 9 (40) (2021) 23243–23255.
[46] G. Li, R. Zhu, A Multisensory Tactile System for Robotic Hands to Recognize Objects, Adv. Mater. Technol. 4 (11) (2019) 1900602.
[47] M. Liu, Y. Zhang, J. Wang, N. Qin, H. Yang, K. Sun, J. Hao, L. Shu, J. Liu, Q. Chen, P. Zhang, T.H. Tao, A star-nose-like tactile-olfactory bionic sensing array for robust object recognition in non-visual environments, Nat. Commun. 13 (1) (2022) 79.
[48] G. Zu, K. Kanamori, K. Nakanishi, J. Huang, Superhydrophobic ultraflexible triple-network graphene/polyorganosiloxane aerogels for a high-performance multifunctional temperature/strain/pressure sensing array, Chem. Mater. 31 (16) (2019) 6276–6285.
[49] S. Zhao, R. Zhu, Electronic skin with multifunction sensors based on thermosensation, Adv. Mater. 29 (15) (2017) 1606151.
[50] Z. Sun, M. Zhu, Z. Zhang, Z. Chen, Q. Shi, X. Shan, R.C.H. Yeow, C. Lee, Artificial intelligence of things (AIoT) enabled virtual shop applications using self-powered sensor enhanced soft robotic manipulator, Adv. Sci. 8 (14) (2021) 2100230.
[51] I. You, D.G. Mackanic, N. Matsuhisa, J. Kang, J. Kwon, L. Beker, J. Mun, W. Suh, T. Y. Kim, J.B.H. Tok, Z.N. Bao, U. Jeong, Artificial multimodal receptors based on ion relaxation dynamics, Science 370 (6519) (2020) 961–965.
[52] L. Beker, N. Matsuhisa, I. You, S.R.A. Ruth, S. Niu, A. Foudeh, J.B. Tok, X. Chen, Z. Bao, A bioinspired stretchable membrane-based compliance sensor, Proc. Natl. Acad. Sci. U. S. A. 117 (21) (2020) 11314–11320.
[53] Y. Qiu, S. Sun, X. Wang, K. Shi, Z. Wang, X. Ma, W. Zhang, G. Bao, Y. Tian, Z. Zhang, H. Ding, H. Chai, A. Liu, H. Wu, Nondestructive identification of softness via bioinspired multisensory electronic skins integrated on a robotic hand, npj Flex, Electron. 6 (1) (2022) 45.
[54] Y. Qiu, Y. Tian, S. Sun, J. Hu, Y. Wang, Z. Zhang, A. Liu, H. Cheng, W. Gao, W. Zhang, H. Chai, H. Wu, Bioinspired, multifunctional dual-mode pressure sensors as electronic skin for decoding complex loading processes and human motions, Nano Energy 78 (2020), 105337.
[55] A. Khasnobish, M. Pal, D.N. Tibarewala, A. Konar, K. Pal, Texture- and deformability-based surface recognition by tactile image analysis, Med. Biol. Eng. Comput 54 (8) (2016) 1269–1283.
[56] H. Liu, Y. Yu, F. Sun, J. Gu, Visual-tactile fusion for object recognition, IEEE T. Autom. Sci. Eng. 14 (2) (2017) 996–1008.
[57] M. Rasouli, Y. Chen, A. Basu, S.L. Kukreja, N.V. Thakor, An extreme learning machine-based neuromorphic tactile sensing system for texture recognition, IEEE Trans. Biomed. Circuits Syst. 12 (2) (2018) 313–325.
[58] E. Kerr, T.M. McGinnity, S. Coleman, Material recognition using tactile sensing, Expert Syst. Appl. 94 (2018) 94–111.